Quaternary Science Reviews 284 (2022) 107496

Contents lists available at ScienceDirect

Quaternary Science Reviews

journal homepage: www.elsevier.com/locate/quascirev

Revised temporal and morphostratigraphic context for Clark Quarry: A late-Pleistocene, fluvially-reworked, Atlantic coast backbarrier deposit

Christopher T. Seminack [a, *], Jesse D. Thornburg [b], Alfred J. Mead [c], Heidi F. Mead [c], Carla S. Hadden [d], Alexander Cherkinsky [d], Michelle S. Nelson [e], David B. Patterson [f]

[a] Lewis F. Rogers Institute for Environmental and Spatial Analysis, University of North Georgia, 3820 Mundy Mill Rd., Oakwood, GA, 30566, USA
[b] Department of Earth and Environmental Science, Temple University, 1801 N. Broad St., Philadelphia, PA, 19122, USA
[c] Department of Biological and Environmental Sciences, Georgia College and State University, 231 W. Hancock St., Milledgeville, GA, 31061, USA
[d] Center for Applied Isotope Studies, University of Georgia, 120 Riverbend Rd., Athens, GA, 30602, USA
[e] Luminescence Laboratory, Utah State University, 1770 N. Research Pkwy., Suite 123, North Logan, UT, 84341, USA
[f] Department of Biology, University of North Georgia, 82 College Cir., Dahlonega, GA, 30597, USA

ARTICLE INFO

Article history:
Received 8 December 2021
Received in revised form
14 March 2022
Accepted 26 March 2022
Available online xxx

Handling Editor: Dr I Hendy

Keywords:
Princess anne terrace
GPR
LIDAR
Textural analysis
IRSL
^{14}C
Pleistocene
Climate dynamics
North America
Geomorphology
Coastal

ABSTRACT

Sediments along the Atlantic Coastal Plain (ACP) of North America have been the focus of numerous paleontological investigations and yielded a diverse array of vertebrate remains; yet the depositional environments associated with their preservation are poorly understood. In this study, we present a multidisciplinary analysis of the depositional environment at Clark Quarry, a late-Pleistocene, fossil-rich locality located within the ACP in Georgia, USA. Clark Quarry is currently positioned 15 km west of the Atlantic Ocean coast and lies within the Princess Anne Terrace, a 100–80 ka paleobarrier-island complex. Fossil-bearing sediments at Clark Quarry are interpreted to have been deposited as a low-energy, fluvial environment that subsequently reworked low-lying terrain of the Princess Anne Terrace backbarrier. Interpretations of digital elevation models (DEM) and infrared stimulated luminescence (IRSL) ages on K-rich feldspar sand grains indicate that this region was an estuarine zone backing (i.e., westward) the Princess Anne paleobarrier island that was subsequently reworked by fluvial activity 68–52 ka. These new interpretations, paired with additional radiocarbon ages from fossil carbonates and overlying soil horizons, indicate that radiocarbon samples may have been influenced by isotopic exchange and should be interpreted as minimum age estimates. Additionally, ground-penetrating radar (GPR) surveys in conjunction with DEM analysis may have captured the subsurface signature of a meandering fluvial system transitioning to a braided style, emphasizing the dynamic nature of this depositional environment. Non-preferential orientation of excavated long bones suggests multidirectional paleoflow, further suggesting a braided stream influence. When considered in conjunction, these data: 1) indicate that Clark Quarry represents a spatially and temporally resolved window into the late-Pleistocene ecosystem in southeastern North America, and 2) suggest that existing radiocarbon data from late-Pleistocene ACP localities should be considered with caution.

1. Introduction

Fossil-bearing localities within the southeastern Atlantic Coastal Plain (ACP) of North America have yielded abundant Pleistocene-aged vertebrate remains (Voorhies, 1971; Hulbert and Pratt, 1998; Mead et al., 2006; Patterson et al., 2012). Although these fossil assemblages have provided important insights into the taxonomy (e.g., Hulbert and Pratt, 1998; Parmley et al., 2020) and ecology (e.g., Noble et al., 2020) of several lineages, a key challenge has been placing them within a precise depositional and temporal context. Many fossils from the region have been collected in association with dredging operations, thereby removing them from their primary geologic context (Hulbert and Pratt, 1998), while others were dated using imprecise biochronological methods (Kurtén and Anderson, 1980).

In this study, we employ a multidisciplinary approach to better understand the temporal and depositional context of a locality

* Corresponding author.
E-mail address: christopher.seminack@ung.edu (C.T. Seminack).

https://doi.org/10.1016/j.quascirev.2022.107496
0277-3791/

called Clark Quarry along coastal Georgia (Fig. 1). This locality preserves *in situ* vertebrate fossils dominated by well-preserved remains of the Columbian mammoth (*Mammuthus columbi*), the giant long-horned bison (*Bison latifrons*; Mead et al., 2006; Patterson et al., 2012; Noble et al., 2020), a wide array of small mammals (Rhinehart, 2021), reptiles, and amphibians (Parmley et al., 2020), as well as estuarine and marine mollusks.

Clark Quarry lies adjacent to the historic Brunswick-Altamaha Canal (Fig. 1), which was first scientifically explored by Sir Charles Lyell in 1846 (Lyell, 1849). Lyell collected several specimens including a proboscidean molar that became the type specimen of *M. columbi* (Falconer, 1857). Clark Quarry is likely within 2 km of Watkin's Quarry (exact location is unknown), which yielded a near-complete skeleton of *Eremotherium* (giant ground sloth; Voorhies, 1971). The similarity, as well as proximity of these two localities indicate that the depositional circumstances at Clark Quarry may be characteristic of the broader region. Early radiocarbon ages of fossils collected at Clark Quarry suggested that sediments were deposited 22.3–19.8 cal ka BP (Mead et al., 2006; Patterson et al., 2012).

2. Regional setting

The ACP is bounded by the Atlantic Ocean to the east, and Precambrian-to-Paleozoic rock along the Blue Ridge and Piedmont physiographic provinces to the west. Surficial sediments decrease in age seaward, ranging from Cretaceous along the fall line to modern at the present-day coast (Lawton et al., 1976). Exquisitely preserved paleobarrier-island complexes in the form of terraces are found along the southeastern ACP, ranging in age from late Pleistocene to Holocene (Hoyt and Hails, 1967; Hoyt et al., 1968; Hails and Hoyt, 1969a, 1969b; Wehmiller et al., 2004; Willis, 2006; Doar and Kendall, 2014). Terraces along the ACP in Georgia were formed by late-Pleistocene sea-level high stands. Included in each terrace are the former barrier island and the backing lower-lying estuary deposits. In total, six Pleistocene terraces are preserved along the ACP in Georgia, from oldest (most landward) to youngest (most seaward): Wicomico, Penholoway, Talbot, Pamlico, Princess Anne, and Silver Bluff (Hoyt and Hails, 1967; Lawton et al., 1976). Relative ages of terraces are based on associated scarp elevation and distance from the coast. This study primarily focuses on the Princess Anne Terrace.

Seaward-draining fluvial systems have continually reworked the ACP landscape. Leigh (2006, 2008) and Leigh et al. (2004) suggest that river systems along the southeastern ACP transitioned from braided to meandering patterns near the Pleistocene-Holocene boundary. Leigh et al. (2004) indicate that the proximal Altamaha-Oconee River (Fig. 1) valley transitioned from a meandering to braided river system as early as 70 ka (Marine Isotope Stage [MIS] 4) and back to meandering 16–14 ka (MIS 2), with braiding being coeval with local aeolian deposit development. The switch to a braided fluvial style was likely caused by an increase in sediment load, channel bank instability, and a punctuated runoff season in response to cooler and drier paleoclimates during this period (Leigh et al., 2004; Leigh, 2006).

3. Local setting

Clark Quarry is located within the ACP, 15 km from the present-day U.S. Atlantic coast, 12 km south of the Altamaha River, and 5 km north of the Turtle River (Fig. 1). Both the Turtle and Altamaha Rivers currently exhibit a meandering style and flow in a general southeast direction, discharging into the Atlantic Ocean. Clark Quarry is located within the backbarrier of the Princess Anne Terrace, 0.5 km landward (west) of the transition to the paleobarrier-island sediments (Hoyt et al., 1968; Ward et al., 1971; Patterson et al., 2012). A wide range of dates for the genesis of the Princess Anne Terrace have been proposed, ranging from 100 to 80 ka (based on uranium disequilibrium series, amino acid racemization, and optically stimulated luminescence; Wehmiller et al., 2004; Willis, 2006; Doar and Kendall, 2014), thereby spanning most of MIS 5 (130–71 ka; Lisiecki and Raymo, 2005). Here, we leverage a multi-disciplinary approach (biologic, geochronologic, sedimentologic, and geomorphic) to establish a more precise age

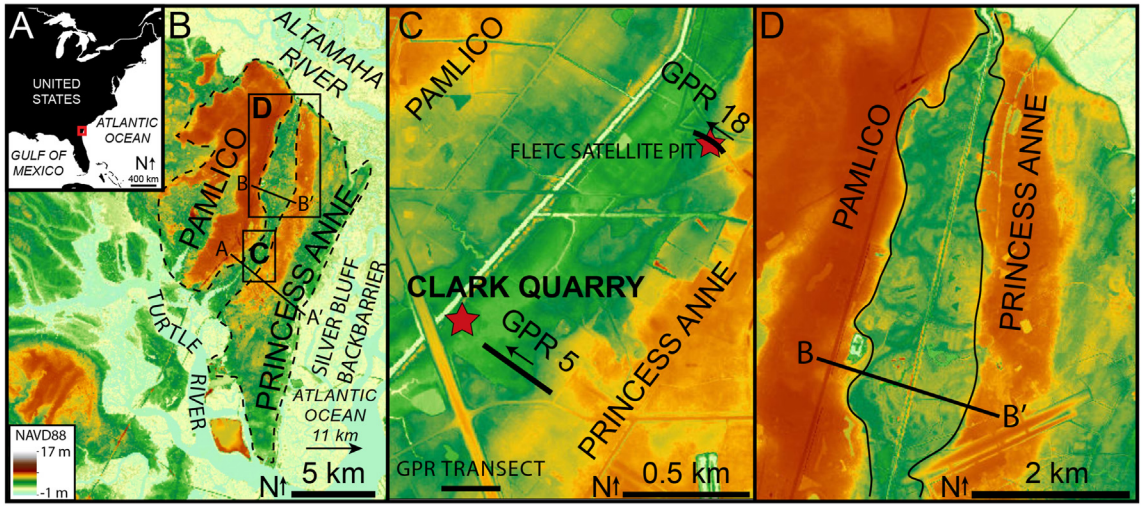

Fig. 1. Digital elevation model (DEM) of the Clark Quarry area. A) Location of Clark Quarry (red box) in relation to the U.S. Atlantic and Gulf of Mexico coasts. B) DEM showing the extent of the barrier-island deposits (dashed line) of the Pamlico and Princess Anne Terraces. Additionally, the extent of panels C and D are outlined, along with the locations of Topographic Profiles A-A′ and B–B′ (see Fig. 3). C) DEM showing the location of Clark Quarry (starred), FLETC satellite pit (starred), the barrier island (higher elevation in the southeast) and backbarrier (lower elevation in the center) portions of the Princess Anne Terrace, in addition to a portion of the Pamlico Terrace barrier island (higher elevation to the northwest). The locations of GPR profiles are displayed with arrows demonstrating the direction data were collected. Clark Quarry is located within the backbarrier portion of the Princess Anne Terrace. D) DEM displaying relict geomorphic features interpreted as a meandering-to-braided fluvial system that once flowed between the Pamlico and Princess Anne paleobarrier islands. Black lines indicate the extent of the fluvially-influenced area. (For interpretation of the references to color in this figure legend, the reader is referred to the Web version of this article.)

control and depositional history for the vertebrate remains associated with Clark Quarry.

4. Methods

4.1. Remote sensing

A digital elevation model (DEM) was analyzed to interpret and identify geomorphic features and their spatial relationship to Clark Quarry. Topographic profiles were constructed using the DEM. The DEM utilized an assemblage of Light Detecting and Ranging (LIDAR) datasets collected by the Coastal Georgia Elevation Project (GCEP; January to March 2010); Chatham County, Georgia (February 2006); Liberty County, Georgia (March 2006); and Glynn County, Georgia (March to April 2001). These data have a vertical resolution of 15 cm, a horizontal resolution of 1 m, and use the North American Vertical Datum of 1988 (NAVD88). It is important to note that 0 m NAVD88 is equivalent to −0.16 m mean sea level (MSL) at Fernandina Beach, FL (National Oceanic and Atmospheric Administration [NOAA] tide gauge 8720030), 63 km south of Clark Quarry (NOAA, 2021).

4.2. Geophysics

A high-resolution ground-penetrating radar (GPR) survey was conducted in the area proximal to Clark Quarry (Fig. 1C) with a GSSI 200 MHz shielded antenna fitted with an SIR 4000 control unit. A total of 3.2 km of GPR transects were collected in general shore-normal and shore-parallel orientations. Much of the data collected was affected by signal attenuation due to a ~1 m thick subsurface mud unit; however, two GPR transects did attain signal penetration depths of 3.5 m or greater. Post-processing including gain restoration, background removal, and a finite impulse response (FIR) filter utilizing a high pass of 145 MHz was performed using the GSSI RADAN 7 software. Because of the complex subsurface stratigraphy, an average dielectric constant (ϵ_r) of 10 (corresponding to a wave velocity of 9.5 cm/ns) was utilized to approximate for depth.

4.3. Trenching and sediment samples

Clark Quarry was excavated to a depth of 2.5 m, where the water table was encountered. Existing excavation width is estimated to be 10 m. In addition to ground-truthing geophysical data, the excavation served as a means of collecting sediment samples for textural analysis, radiocarbon, and luminescence dating. Excavation sidewalls were photographed, and the underlying shallow stratigraphy was visually described in terms of color, sediment size, sedimentary structures, mineralogy, and biological content (Fig. 2).

Stratigraphic units consisting of fine-grained sediment (i.e., clay- and carbonate-rich units) were documented by visual description in the field. Soil horizons were identified following the United States Department of Agriculture (USDA) soil taxonomy nomenclature (Soil Survey Staff, 2014). Sediment samples were collected from the sand-dominated stratigraphic units for textural analysis. Sand samples were desiccated and disintegrated at the University of North Georgia Sedimentology Laboratory. Samples were split using a Homboldt Riffle-Type Sample Splitter into 10–20 g sample sizes and sieved at 0.25 ϕ intervals with a Gilsonic AutoSiever Sonic Sifter. Textual analysis of sand samples followed the methods described by Folk (1980). Statistics were calculated using the GRADISTAT macro for Microsoft Excel (Blott and Pye, 2001) and utilized the Folk and Ward method for mean, sorting, and skewness (Folk and Ward, 1957).

4.4. Bone orientation

Fluvial processes can preferentially orient fossil remains (Toots, 1965a, 1965b; Voorhies, 1969; Lyman, 1994). Variables such as the ratio between channel width and bone length/shape, articulated versus disarticulated bones, and the makeup of channel thalweg may affect bone orientation upon burial in a channel (Voorhies, 1969; Hanson, 1980; Frison and Todd, 1986; Lyman, 1994). Specifically, streamflow tends to orient long bones with a heavier end (e.g., limbs and thoracic vertebrae) parallel to the direction of flow, while bones with equally distributed weight (e.g., ribs) tend to orient their long axis perpendicular to streamflow direction (Voorhies, 1969; Lyman, 1994). Shipman (1993) recommends at least 72 bone measurements be utilized in a paleoflow study to account for bone orientations that are not a function of fluvial activity (e.g., trampling). In total, 72 inclination and orientation measurements of *M. columbi* and *B. latifrons* limb bones (n = 16), thoracic vertebrae (n = 16), and ribs (n = 40) were collected during excavations at Clark Quarry (see Fig. 2A for an image of *in situ B. latifrons* bones within the excavation and Fig. 2C for the stratigraphic context of the fossiliferous unit). Mirrored rose diagrams (Shipman, 1993; Lyman, 1994; Martin, 1999) were constructed using orientation measurements of bones to determine flow direction during their burial at a grid interval of 5°.

4.5. Radiocarbon dating

Five fossil samples were collected for ^{14}C dating by accelerator mass spectrometry (AMS). These samples consisted of bone (*B. latifrons*) and shell (eastern oyster, *Crassostrea virginica*) material. Samples were collected via excavation. Bone bioapatite was analyzed following Cherkinsky (2009) due to the lack of collagen preservation. Additionally, 11 soil and sediment samples from above the fossil horizon were collected for ^{14}C dating by AMS. Sample analyses were conducted at the Center for Applied Isotope Studies at the University of Georgia following standard laboratory procedures (Cherkinsky et al., 2010). Results were calibrated in OxCal version 4.4 (Ramsey, 2021) using the IntCal20 curve (Reimer et al., 2020) for terrestrial samples and the Marine20 curve (Heaton et al., 2020) for marine samples. A reservoir correction (ΔR) of −286 ± 68 years was obtained from an average of nine ΔR values from St. Catherines Island, GA, USA (Thomas, 2008), and applied to marine mollusk shell samples.

4.6. Infrared stimulated luminescence dating

Luminescence dating provides an age estimate of the last exposure of minerals (typically quartz or feldspar) to light or high heat (Aitken et al., 1964; Huntley et al., 1985). Following burial or removal from heat, ionizing radiation from the surrounding sediments and incident cosmic radiation leads to the accumulation of trapped charge (ionized electrons) within defects in the mineral-lattice (Aitken, 1998). This stored energy is released as luminescence (photons of light) when exposed to controlled light or heat conditions in the luminescence laboratory. The intensity of the luminescence signal corresponds to the amount of radiation absorbed over time (following a linear function that becomes saturating exponential at higher doses) and is related to the radioactivity of the sample site (Aitken, 1998). The laboratory dose required to reproduce the natural dose (burial dose) is known as the D_E (equivalent dose, reported in Gy). The environmental radioactivity of the sample site is known as the D_R (dose rate, reported in Gy/kyr). The age is calculated by dividing the D_E by the D_R.

In this study, infrared stimulated luminescence (IRSL) dating on K-rich feldspar sediment (125–212 μm) was performed on five

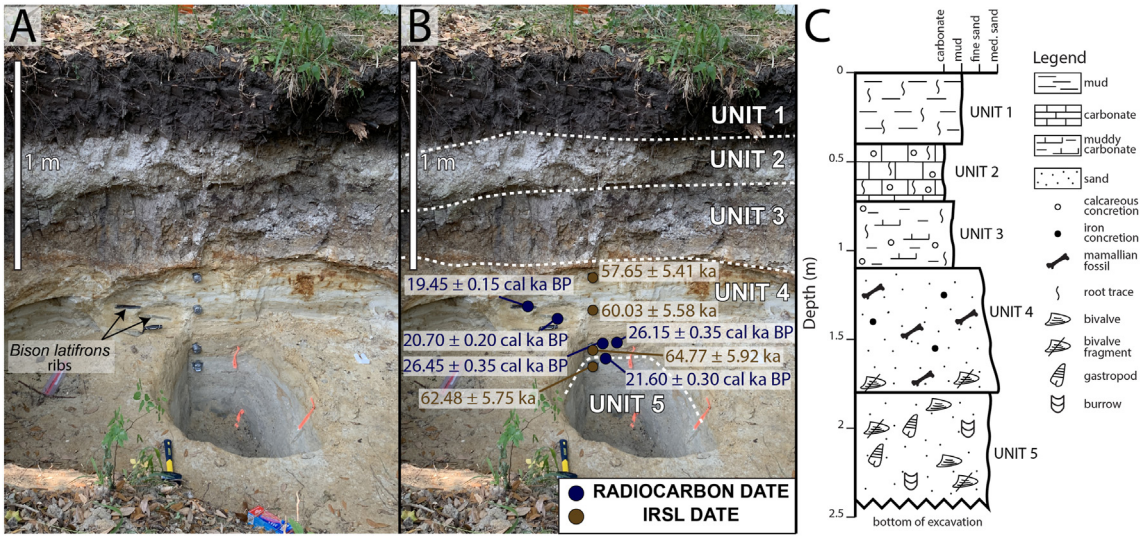

Fig. 2. Image and interpretation of the Clark Quarry excavation. A) Uninterpreted image of the excavation; location of *Bison latifrons* rib fragments highlighted. B) Image of the excavation overlain with facies interpretations, mammal and mollusk radiocarbon sample locations and ages, and IRSL sample locations and ages. Fossils are found in Unit 4, which is interpreted as fluvial in origin. Unit 5 is interpreted as the backbarrier environment of the Princess Anne Terrace. C) Stratigraphic column describing the lithology of the excavation at Clark Quarry.

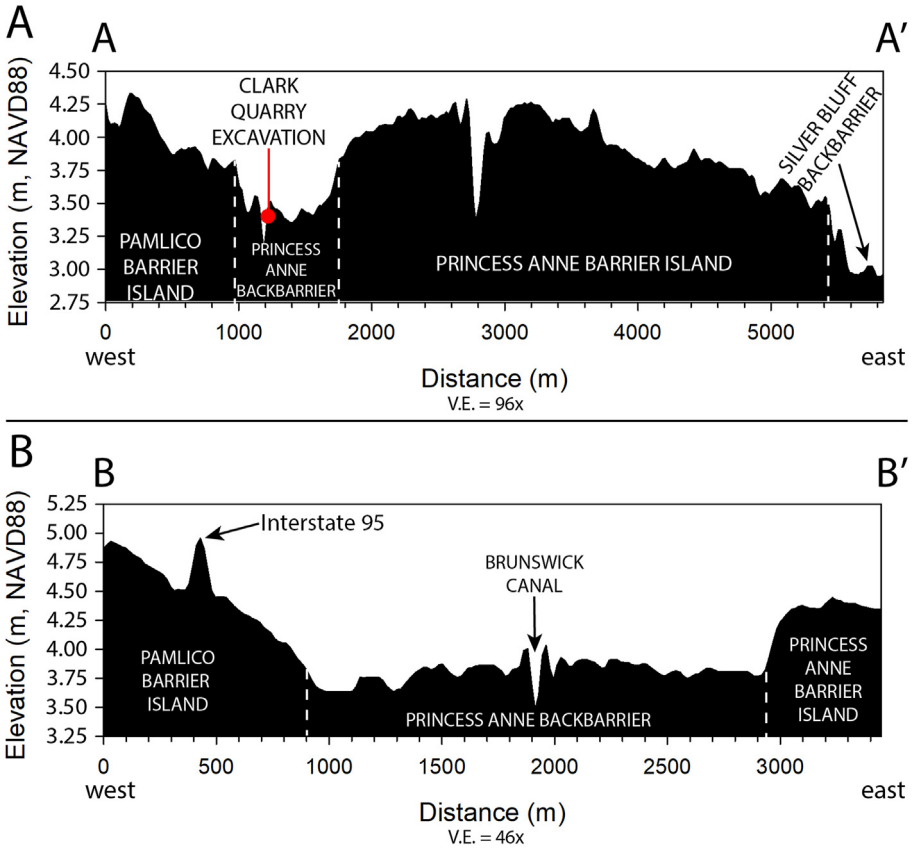

Fig. 3. Topographic profiles of the Pamlico and Princess Anne Terraces, in addition to the low-lying area separating the two paleobarrier islands. See Fig. 1B for the location of the topographic profiles. V.E. = vertical exaggeration. A) Topographic Profile A-A′ extending across the eastern portion of the Pamlico Terrace, Clark Quarry, the entire Princess Anne Terrace, and the western portion of the Silver Bluff Terrace. Dashed white lines distinguish the approximate boundary of former barrier island and backbarrier environments. B) Topographic Profile B–B′ is situated 6.8 km north of Clark Quarry. Dashed white lines distinguish the approximate boundary of former barrier island and backbarrier environments. Note the undulating topography displaying hypothesized channels and interfluves within the fluvial sediments, just west of the Brunswick Canal.

samples. Four samples were collected from the main excavation (CQ-19-1, CQ-19-2, CQ-19-3, CQ-19-4; Fig. 2) and one sample was obtained from the FLETC satellite pit 1.2 km northeast of Clark Quarry (FLETC-OSL-1-19-155cm; Fig. 1). Each IRSL sample contained three subsamples, the D_E sample, the D_R sample, and a water content sample collected in an airtight container. Samples for D_E

analyses were collected at the trench sidewall in 3.8-cm by 20.3-cm opaque metal tubes (so as not to expose the sample to light), and the D_R sample was collected from sediments within a 30-cm radius of the D_E sample in a plastic bag. Water content samples were collected after tube extraction from as far back into the trench wall as possible to avoid desiccation effects at the exposure.

The five sediment samples were processed and analyzed at the Utah State University Luminescence Laboratory in North Logan, Utah. D_E sample tubes were opened under dim amber light (~590 nm) and ~3 cm of potentially light-exposed material from the outer ends of tubes was removed and discarded prior to further processing. The remaining sediment was then wet sieved to a target grain-size range (125–212 μm), treated with 10% hydrochloric acid and hydrogen peroxide to dissolve carbonates and organic material, respectively. Feldspar grains were twice separated from higher density minerals using sequential 2.7 g/cm^3 and 2.58 g/cm^3 a heavy liquid sodium polytungstate solution, and dried at room temperature (Wintle, 1997).

Luminescence measurements were made on K-rich feldspar sand grains following the IRSL single-aliquot regenerative dose (SAR) method of Wallinga et al. (2000) on 1-mm multi-grain aliquots (~5–10 grains per aliquot). Infrared measurements were performed on Risø TL/OSL Model DA-20 readers with infrared light-emitting diodes (LEDs; 870 ± 40 nm) and reader dose rates of 0.10 Gy/s from a decaying ^{90}Sr beta source (Bøtter-Jensen et al., 2003). The luminescence signal was measured through a blue filter pack of 2-mm and 4-mm thick filters (BG-39 and Corning 7–39, respectively) over 100 s (250 channels) at 50° C with LED diodes at 85% power (~120 mW). The resultant signal was calculated by subtracting the average of the last 10 s (chnls 225–250; background signal) from the first 0.8 s (chnls 1–2; peak signal) of the signal decay curve. Preheat conditions prior to natural, regenerative and test dose signals were at 250° C, held for 60 s (Blair et al., 2005). Dose response curves were fit within saturating-exponential and saturating-exponential plus linear fits to calculate individual aliquot D_E values.

The IRSL ages were calculated by correcting individual D_E measurements for fading (loss of signal with time, g2days %/decade) using the method of Auclair et al. (2003) and the age correction model of Huntley and Lamothe (2001). Cumulative D_E and IRSL age values were calculated using the Central Age Model (CAM) of Galbraith and Roberts (2012). Only one out of all aliquots run (75 total between 5 samples) was rejected from further analyses because the natural D_E value was greater than the highest regenerative laboratory dose given. Uncertainty on D_E estimates are reported at 2-sigma standard error and 1-sigma standard error for the IRSL age. Random and systematic uncertainties include instrument calibration, and dose rate and equivalent dose calculations and were calculated in quadrature using the methods of Aitken and Alldred (1972) and Guérin et al. (2011).

D_R samples were dried, homogenized, and analyzed for radioisotope concentration of K, Rb, Th, and U using ICP-MS and ICP-AES techniques. These concentration values were converted to alpha, beta, and gamma dose rates using conversion factors from Adamiec and Aitken (1998) and Guérin et al. (2011). Internal beta dose rate from K was added to the dose rate calculation, assuming a mineral composition of 12.5% K on feldspar grains (following Huntley and Baril, 1997), and attenuated to water content and grain size using factors outlined by Mejdahl (1979) and Aitken (1985). For the internal Rb content, we assumed 400 ppm following Huntley and Hancock (2001) and attenuated the internal beta dose rate to water content. Finally, due to the lack of etched edges on the feldspar grains, an alpha effectiveness value ('a-value') is used to correct the saturated nature of traps along highly ionizing alpha tracks (Aitken, 1985). We assume an alpha efficiency of 0.086 ± 0.009 following Rees-Jones (1995) in the alpha contribution to the total dose rate. Contribution of cosmic radiation to the dose rate was calculated using sample depth, elevation, latitude, and longitude following Prescott and Hutton (1994). Total dose rates were calculated based on water content, radioisotope concentrations, and cosmic dose rate (Aitken and Xie, 1990; Aitken, 1998; Adamiec and Aitken, 1998).

4.7. Constraining IRSL age uncertainties

The principle of superposition was utilized to constrain the uncertainties associated with age-dating samples. Therefore, the age range of each sample will continually decrease upwards in the section, assuming the lack of significant sedimentological mixing. The mean age and uncertainty range was plotted for each sample according to depth. Age uncertainty ranges were truncated if a portion of the overlying sample was older than the uncertainty range of the underlying sample, or if a portion of the underlying sample uncertainty range was younger than the uncertainty range of the overlying sample. This method was utilized to further constrain the timing of deposition withing the stratigraphic column.

5. Results

5.1. Remote sensing

Clark Quarry is located within the former backbarrier environment (i.e., western side) of the Princess Anne Terrace based on the geomorphic interpretation of the DEM (Fig. 1B and C). Backing the Princess Anne Terrace (further westward) is the Pamlico Terrace. A series of relict meandering-to-braided channels in a general north-south orientation between the two paleobarrier islands are present in the DEM, north of Clark Quarry (Fig. 1D).

Topographic profile A-A′ represents a northwest-southeast oriented transect from the seaward (eastern) portion of the Pamlico barrier island and across the entire Princess Anne Terrace (Figs. 1B and 3A). The profile intersects the study site at the 1,200 m mark in the profile. Within this profile, the Pamlico barrier island deposits reach a maximum elevation of 4.33 m (NAVD88), then decrease to 3.82 m seaward (east). The Pamlico barrier island transitions to the Princess Anne estuarine platform at the 970 m mark along A-A'. The estuarine platform of the Princess Anne Terrace is found between the 970 and 1,750 m marks of Profile A-A'. Clark Quarry is located near the center of the estuarine platform. It should be noted that Profile A-A′ intersects the Brunswick Canal (3.13 m elevation) at the 1,180 m mark in the transect. The elevation of Profile A-A′ increases on the Princess Anne barrier island to a maximum of 4.28 m. The Princess Anne barrier island has a width of 3,600 m along Profile A-A'. Generally, Profile A-A′ displays the Princess Anne barrier island as asymmetrical in shape, with topography dipping to the southeast. The backbarrier portion of the Silver Bluff Terrace is displayed between the 5,420 m mark and the eastern terminus of Profile A-A' (5,840 m mark), exhibiting undulating topography near 3.00 m in elevation.

Topographic Profile B–B′ displays the terrain 4 km north of Clark Quarry (Fig. 1B, D, and 3B), within the vicinity of the hypothesized former braided channel-like features, in a northwest-southeast orientation. The profile extends from the easternmost portion of the Pamlico barrier island, across the Princess Anne Terrace backbarrier platform, to the westernmost portion of the Princess Anne barrier island (Fig. 1B, D, and 3B). Within this topographic profile, the Pamlico barrier island reaches a natural topographic high of 4.90 m at the 32 m mark. Another topographic high is observed at the 412 m mark for U.S. Interstate Highway 95 (Fig. 3B). Elevation

decreases from the 32 m point to the seaward terminus of the Pamlico barrier island at the 900 m mark. The Princess Anne Terrace backbarrier platform is displayed between the 900 and 2,930 m marks and has an undulating surficial expression ranging from 3.63 to 4.03 m in elevation. Profile B–B′ intersects the Brunswick Canal at the 1,910 m mark. The slight topographic highs on either side of the canal are likely dredge spoils associated with its construction. Finally, Topographic Profile B–B′ intersects the Princess Anne barrier island at the 2,930 m mark and continues to the eastern terminus of the profile at the 3,446 m mark. Elevation of the Princess Anne barrier island reaches a maximum of 4.44 m at the 3,231 m mark.

5.2. Geophysics

GPR Profile 5 was collected 0.5 km southeast of Clark Quarry and had signal penetration of approximately 3.5 m (Figs. 1C and 4). At least seven shore-parallel channel features were interpreted within the 105 m profile (Fig. 4B). The radargram reveals a complex system of small, overprinted channels ~15–20 m in width. A larger 47-m wide channel was imaged between the 8 and 55 m marks of the transect. This is interpreted as a younger channel because it cuts across adjacent channels. A larger channel was also imaged at the easternmost portion of the profile (80–105 m markers); however, the eastern boundary, as well as the bottom of the channel were not imaged within the radargram.

GPR Profile 18 was located 1.3 km northeast of Clark Quarry and had signal penetration of approximately 6 m (Figs. 1C and 5). Many paleochannels were interpreted in the radargram. All channels (except one) have a width of 10–20 m and a scouring depth of approximately 3 m. A larger paleochannel was imaged along the bottom half (below a depth of 3 m) of the profile. The floor of this paleochannel was not imaged in the radargram, and thus the depth of maximum scour exceeds 6 m. Easterly-dipping clinoforms are imaged from 3 to 6 m in depth, west of the larger lower paleochannel (5–65 m marks), as well as westerly-dipping clinoforms at a similar depth to the east (95–120 m marks).

5.3. Trenching and sediment samples

The excavation at Clark Quarry extends 2.5 m below the surface and is limited in depth by the presence of groundwater (Fig. 2). Five stratigraphic units were identified within the excavation (Fig. 2B and C). Units 1 through 3 are soil horizons. Unit 1 represents the O-Horizon extending from a depth of 0–0.40 m. Unit 2 is a B_k-Horizon spanning from 0.40 to 0.72 m. Unit 3 represents the B_k/C-Horizon extending from 0.72 to 1.09 m. Unit 4 is a fossil-rich unit consisting of tan-colored, fine quartzose sand, interspersed with iron nodules extending from 1.09 to 1.80 m of the excavation. Three shell hash lenses span horizontally along the bottom 0.30 m of the unit. No other sedimentary structures were identified within Unit 4. Unit 5 is greenish-gray, fine quartzose sand that spans from 1.80 m to the bottom of the excavation (~2.5 m). The bottom of Unit 5 was not unearthed. This unit contains abundant intact and fragmented bivalves (*Crassostrea virginica)*, fragmented and intact gastropods (*Ilyanassa obsoleta*), and some vertical burrows. No terrestrial fossils were present within this unit.

Textural analysis was performed on sandy Units 4 and 5 (Fig. 6). Mean grain-size analysis indicated that all samples were within the fine sand size class; however, two general vertical grain-size trends were apparent (Fig. 6A). Samples from the lowest extent of the excavation, 210 cm–170 cm, show little fluctuation in grain size, with all samples nearly 2.8 φ (0.14 mm) in diameter. Samples from 160 to 100 cm display a fining-upward succession; mean grain size decreases from 2.2 φ (0.22 mm) at 160 cm to 2.7 φ (0.15 mm) at 100 cm.

Textural analysis reveals two vertical trends in sorting (Fig. 6B). Samples from 210 to 170 cm yielded similar results, straddling the well sorted and very-well sorted categories. A sharp decrease in sorting occurs between the 170 and 160 cm samples, decreasing from very-well sorted to moderately sorted, respectively. Samples from 150 cm to 100 cm increase slightly in sorting upward, with values in the moderately sorted category.

Finally, two vertical trends are apparent in the skewness results from the excavation. Sediment samples from 210 to 170 cm exhibit near symmetrical skewness and increase in value to fine skewed at 170 cm. Skewness values decrease sharply at 160 cm to the strongly coarse skewed category. Finally, skewness values gradually increase upwards to near symmetrical at the top of the sand units at 100 cm.

5.4. Bone orientation

M. columbi and *B. latifrons* limbs, thoracic vertebrae, and ribs did not display a definitive preferred orientation. Weak evidence of alignment may be apparent in the east-southeast to west-northwest direction, (Fig. 7A). Additionally, some nearly north-to-south alignment is occurring for rib bones (Fig. 7B).

5.5. Age dating

The two chronometric techniques (IRSL and radiocarbon) utilized in this study yielded varying results (Tables 1 and 2). IRSL

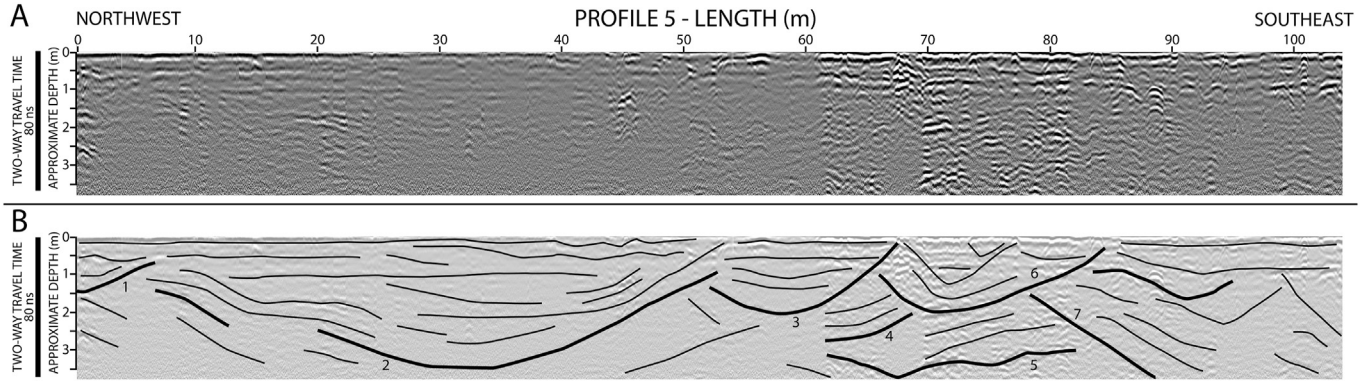

Fig. 4. GPR data showing multiple overprinted channels. Data were collected 0.5 km southeast of Clark Quarry. A) Uninterpreted GPR data. B) Interpreted GPR data. The radargram shows a series of at least seven stacked paleochannels within a 105 m span. The largest channel has a width of 50 m and a depth of 3.5 m. Interpreted flow for these channels is to the south, towards the Turtle River. Channels floors are delineated by numbered bolded line tracings.

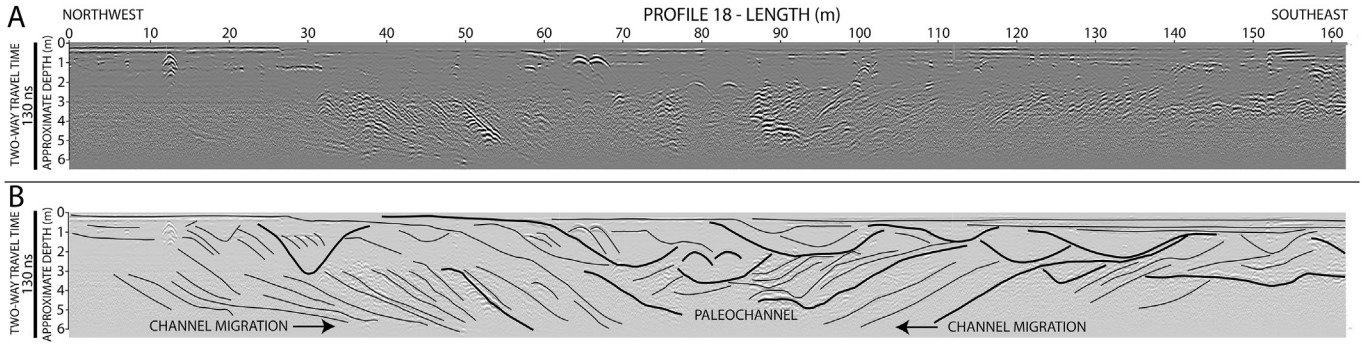

Fig. 5. GPR data showing a change in fluvial style from meandering to braided. Data were collected 1.3 km southeast of Clark Quarry within the paleoestuary of the Princess Anne Terrace. A) Uninterpreted GPR data. B) Interpreted GPR data. This radargram displays a larger, deeper channel between the 60- and 110-m marks, scouring more than 4.5 m below the surface. The larger channel appears to have been meandering in a back-and-forth motion as evidenced by opposing clinoform on either side of the channel floor. Multiple smaller, shallower channels overprint the deeper channel between approximated depths of 0–3.5 m. This radargram likely captures the transition from a meandering to braided fluvial style. Channels floors are delineated by bolded line tracings.

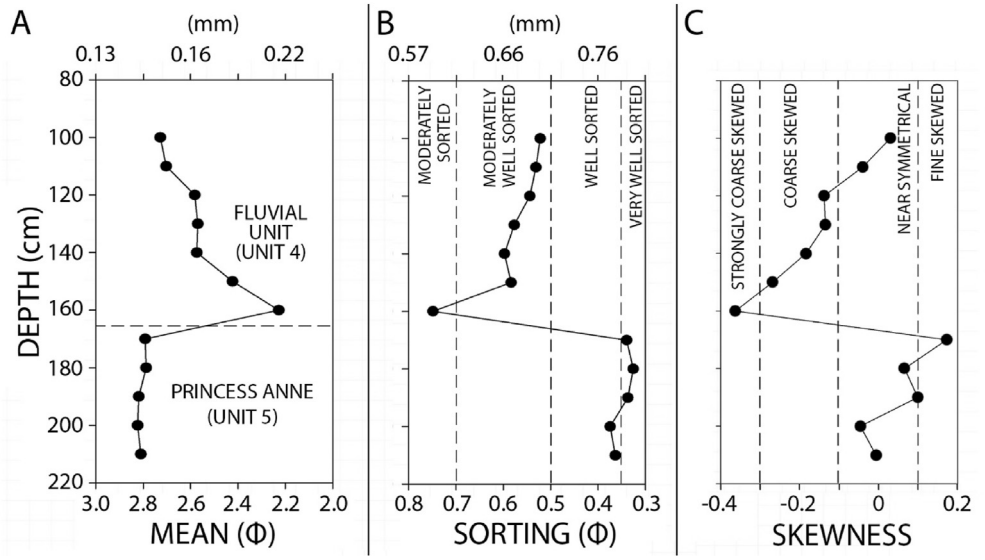

Fig. 6. Textural analysis of the quartzose-dominated, sandy Units 4 and 5 at Clark Quarry. A) Mean grain size versus depth. The overlying fluvial unit displays a fining-upward succession. B) Sorting versus depth. C) Skewness versus depth.

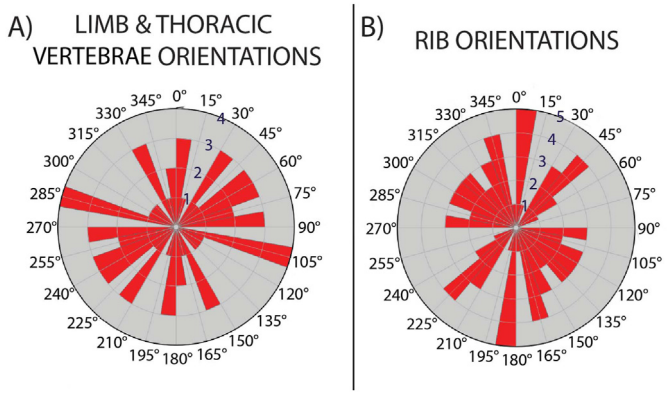

Fig. 7. Mirrored rose diagrams of excavated *Mammuthus columbi* and *Bison latifrons* A) limbs (n = 16) and thoracic vertebrae (n = 16), and B) ribs (n = 40) from Clark Quarry.

samples generally decrease in age upward through the stratigraphic section (Table 1; Fig. 8A). Samples from the Clark Quarry excavation resulted in a cluster of consecutively overlapping dates ranging from 68.23 to 52.24 ka, while the satellite pit sample collected lateral to Clark Quarry (FLETC-OSL-1-19) yielded a date of 53.93 ± 5.20 ka (Table 1; Figs. 1C and 8A). Sample CQO-19-3 does imply a slightly older age than CQO-19-4 (64.77 ± 5.92 ka vs. 62.48 ± 5.75 ka, respectively), despite being collected 15 cm above CQO-19-4. These two samples were likely penecontemporaneous, which explains the large overlap with the shallower sample exhibiting the older mean age. The three IRSL ages from stratigraphic Unit 4 at Clark Quarry and the IRSL age from the FLETC satellite pit are interpreted as a fluvial depositional setting and have a common overlap window of 59.13–58.85 ka based on sample uncertainty truncations. More details on D_E distribution, D_R chemistry, and luminescence properties are available in the supplemental section (Table S1; Figure S1).

Direct radiocarbon dates on fossil samples collected from the same sandy stratigraphic Units 4 and 5 resulted in a separate non-overlapping population of dates, which are significantly younger compared to the IRSL samples. These dates spanned from 28.6 to 19.3 cal ka BP (Table 2; Fig. 8B). Radiocarbon ages on soils and sediments overlying the fossil bed (Units 1–3) are younger overall, and ages generally increase with depth, with some notable stratigraphic reversals.

Table 1
Infrared stimulated luminescence (IRSL) age information.

Sample num.	USU num.	Num. Of aliquots[a]	Sample Depth (m)	Dose rate (Gy/ka)	Fading Rate g_{2days} (%/decade)	Equivalent Dose[b] ± 2σ (Gy)	IRSL age[c] ± 1σ (ka)
CQO-19-1	USU-3090	14 (14)	1.27	3.54 ± 0.19	1.87 ± 0.30	171.83 ± 11.30	**57.65 ± 5.41**
CQO-19-2	USU-3091	12 (13)	1.47	3.87 ± 0.21	1.58 ± 0.15	201.22 ± 11.59	**60.03 ± 5.58**
CQO-19-3	USU-3092	16 (16)	1.72	2.86 ± 0.15	1.19 ± 0.08	166.17 ± 9.64	**64.77 ± 5.92**
CQO-19-4	USU-3093	16 (16)	1.87	3.29 ± 0.17	1.23 ± 0.14	183.77 ± 10.43	**62.48 ± 5.75**
FLETC-OSL-1-19-155cm	USU-3094	16 (16)	1.55	4.46 ± 0.26	1.59 ± 0.04	208.21 ± 12.99	**53.93 ± 5.20**

[a] Age analysis using the single-aliquot regenerative-dose procedure of Wallinga et al. (2000) on 1-mm small-aliquots of feldspar sand (125–212 μm) at 50 °C IRSL. Number of aliquots used in age calculation and number of aliquots analyzed in parentheses.
[b] Equivalent dose (D_E) and IRSL age calculated using the Central Age Model (CAM) of Galbraith and Roberts (2012).
[c] IRSL age on each aliquot corrected for fading following the method by Auclair et al. (2003) and correction model of Huntley and Lamothe (2001).

Table 2
Ages and descriptions of ^{14}C samples. Calibrated ages rounded to nearest hundred.

SAMPLE ID	DEPTH (m)	MATERIAL	$\delta^{13}C$ (‰ VPDB)	^{14}C YR BP	CAL YR BP 95% PROBABILITY RANGE
Soils/sediments					
CQ-RAD-A1	0–.02	A1 soil, bulk organics	−27.2	modern	0
CQ-RAD-A1	.08–.12	A1 soil, bulk organics	−26.9	160 ± 20	300–0
CQ-RAD-A1	.26–.30	A1 soil, bulk organics	−23.2	1,710 ± 20	1,700–1,500
CQ-RAD-Abc	.35–.37	ABc soil, bulk organics	−22.9	1,910 ± 20	1,900–1,700
CQ-RAD-Bc	.52–.55	Bc soil, bulk organics	−26.4	1,630 ± 20	1,600–1,400
concretion	.62–.68	carbonate concretion	−10.5	3,780 ± 25	4,300–4,000
CQ-RAD-Bc2Ab	.77–.82	Bc2AB buried soil, bulk organics	−24.5	3,390 ± 25	3,700–3,500
CQ-RAD-2Ab	.86–.90	2AB buried soil, bulk organics	−25.3	5,520 ± 30	6,400–6,200
CQ-RAD-2AB	1.00–1.05	2AB buried soil, bulk organics	−23.9	5,980 ± 30	7,000–6,700
CQ-RAD-2Bf	1.22–1.25	2Bf buried soil, bulk organics	−25.5	5,820 ± 30	6,800–6,500
CQ-RAD-2BfC	1.42–1.45	2BfC sediment, bulk organics	−26.2	3,020 ± 30	3,400–3,000
Fossils					
1-6-3-19 b	1.33	*B. latifrons* rib, bioapatite	−6.5	16,150 ± 40	19,600–19,300
1-6-3-19a	1.45	*B. latifrons* rib, bioapatite	−6.5	17,140 ± 40	20,900–20,500
CQ-RAD-5	1.77	mollusk shell	−1.6	24,490 ± 60	26,500–25,800
CQ-RAD-2	1.79	mollusk shell	−1.7	24,790 ± 60	26,800–26,100
CQ-RAD-1	1.86	mollusk shell	−2.4	20,090 ± 50	21,900–21,300

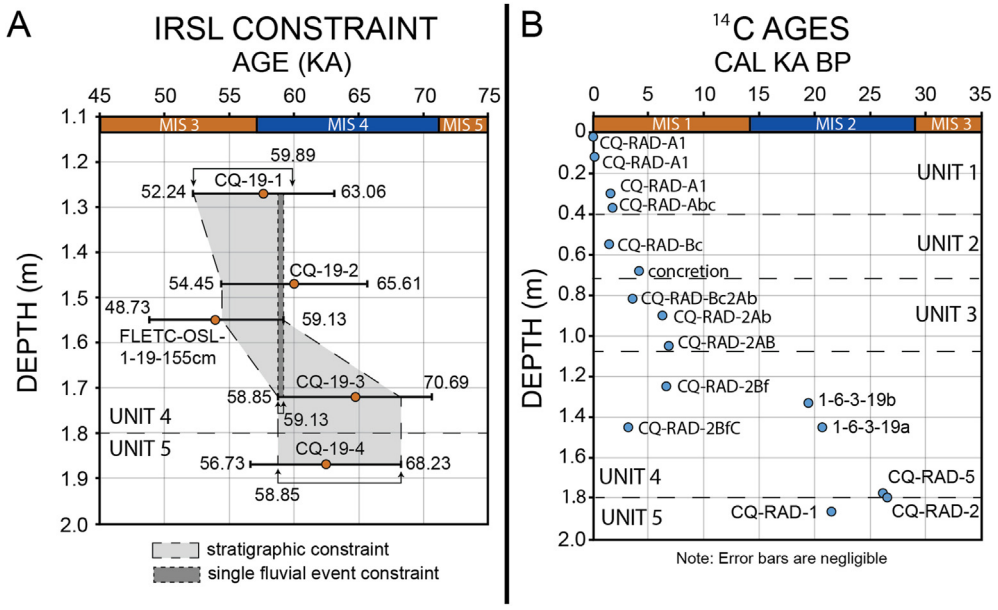

Fig. 8. Chronometric results. A) IRSL sample results with multiple age constraints. CQ-19-1, CQ-19-2, CQ-19-3, and CQ-19-4 were collected from the Clark Quarry excavation. FLETC-1-19-155 cm was collected from the FLETC satellite pit (Table 1; Fig. 1C). B) Radiocarbon results. The vertical stratigraphic discrepancy of radiocarbon dates may have been caused by younger carbon contamination. Please note the difference in depth scale between pane A and B. See Table 2 for radiocarbon dates.

6. Discussion

6.1. Evidence of a fluvial environment

The DEM and topographic profiles indicate a low-lying area between the Pamlico and Princess Anne paleobarrier islands. Previous studies (Hoyt and Hails, 1967; Hails and Hoyt, 1969b; Lawton et al., 1976) suggest this low-lying terrain is representative of the backbarrier environment of the Princess Anne Terrace. Our results indicate: 1) fluvial reworking resulted in sediment deposits that are currently overlying the backbarrier sediments within this localized segment of the Princess Anne Terrace, and 2) the northern segment of this depositional space between the Pamlico and Princess Anne paleobarrier islands is dominated by a meandering-to-braided fluvial pattern (Fig. 1B and D). These findings are consistent with existing studies (Ivester and Leigh, 2003; Leigh et al., 2004; Leigh, 2006, 2008) that indicate the adjacent Altamaha River has a history of switching between meandering and braided styles ultimately based on climatic conditions during late-Pleistocene glaciations. We interpret the fossiliferous stratigraphic unit (Unit 4, Fig. 2B) at Clark Quarry to be of fluvial origin because of lack of *in situ* brackish and marine fossils, abundance of terrestrial mammalian fossils, lack of peat or vegetative material, vertical textural trends (indicating likely sheet sands), DEM data, and GPR interpretations. Additionally, at the time of deposition, Clark Quarry would have been situated ~150 km landward of the shoreline, based on late-Pleistocene sea-level data from Hine et al. (2017). Therefore, this fluvial system would have been dominated by inland fluvial processes, not coastal processes. The geometry of these relict channels suggests a general southward direction of flow between the Pamlico and Princess Anne paleobarrier-island complexes (Fig. 9). This is consistent with the general southeast direction of flow in the contemporary depositional environments in the region, especially tributaries of major rivers that are situated in low-lying terrain, between the topographic highs of paleobarrier islands. Mirrored rose diagrams constructed from bone orientation data are consistent with an east-west dominated flow orientated stream (limbs and thoracic vertebrae orientated east-southeast to west-northwest, ribs nearly normal at a north-south orientation); however, these results are not definitive (Fig. 7). Two possibilities may explain these weakly preferentially orientated bones: 1) a braided stream would show evidence of multiple directions of localized streamflow because of the interweaving and highly dynamic nature of the fluvial style, and 2) the number of bone orientations measured is at the lower limit (n = 72) of what Shipman (1993) suggests for a paleoflow study utilizing elongated bone material.

GPR profiles (Figs. 4 and 5) display multiple stacked and overprinted paleochannels. Fig. 4 displays at least seven in-filled paleochannels, with the largest being 50 m wide and approximately 3.5 m in depth. Potentially larger channels may be present at deeper depths but are not fully imaged in the radargram. Fig. 5 displays a single, larger channel approximately 60 m wide, scouring more than 6 m below the surface. This channel appears to have meandered, apparent by clinoforms between 3 and 6 m in depth dipping in both the east and west directions. Additionally, multiple smaller channels (10–20 m in width, 2–3 m in depth), interpreted as a braided fluvial style, overly the single larger channel. This configuration of channel stacking may have captured the morphostratigraphic signature of the stream system switching from an older meandering style to a younger braided style.

Trenching, visual descriptions, and textural analysis of the shallow subsurface suggests a definitive distinction between the lower sandy Units 4 and 5 (Figs. 2 and 6). Unit 5 is the bottommost exposed unit and is interpreted as backbarrier deposits associated

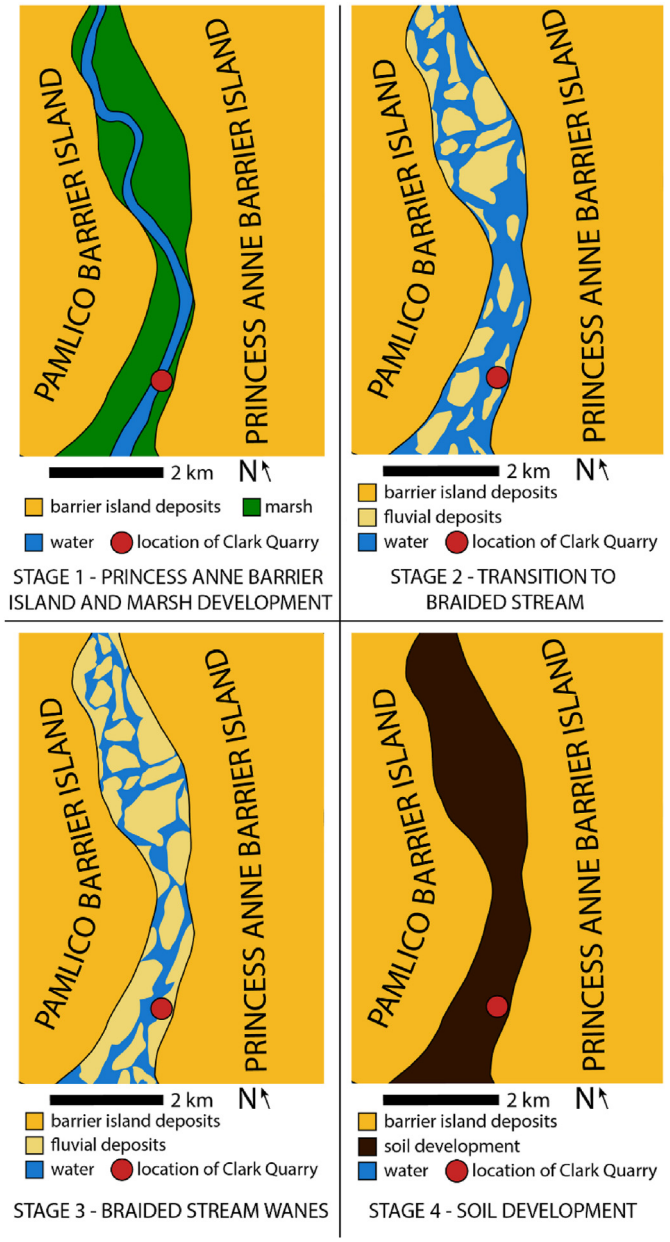

Fig. 9. Proposed evolutionary model of Princess Anne Terrace estuarine environment and Clark Quarry. A) Stage 1 occurred 100–80 ka during the formation of the Princess Anne Terrace, based on previous work (Wehmiller et al., 2004; Willis, 2006; Doar and Kendall, 2014). The backbarrier at this time was likely characterized by a meandering tidal creek within marsh. B) Stage 2 is marked by the transition from meandering tidal creek and marsh to a braided stream 68.23–58.85 ka. C) Stage 3 represents the waning and infilling of the braided stream system, ending by 52.24 ka. D) Stage 4 occurred a minimum of 7 ka as soil development took place overlying the fluvial sediments.

with the Princess Anne Terrace. A change in sediment color, preserved fauna, and sediment texture is observed at approximately 170 cm in depth and likely indicates a switch to a fluvial depositional environment due to the fining-upward succession in grain size, and the sediment being less sorted and more coarsely skewed relative to the underlying Unit 5 (Fig. 6). Therefore, Unit 4 is interpreted as sheet sands of small channels with no distinctive structure indicative of lateral accretion by a shallow braided fluvial system (Miall, 2010).

The fluvial unit thickens laterally in an eastward direction, from Clark Quarry to the locations of the GPR profiles and indicates that

Clark Quarry may have been representative of a flood plain or braid bar environment when deposited, in contrast to the GPR profiles displaying the deeper scoured channels. Trample marks and evidence of scavenger gnaw-marks on the *B. latifrons* bones suggest that their skeletons were exposed subaerially for some amount of time before burial (Fig. 10). We hypothesize that vertebrate remains were entrained by a flooding event (possibly exacerbated by the variable discharge nature of braided streams) and buried within the

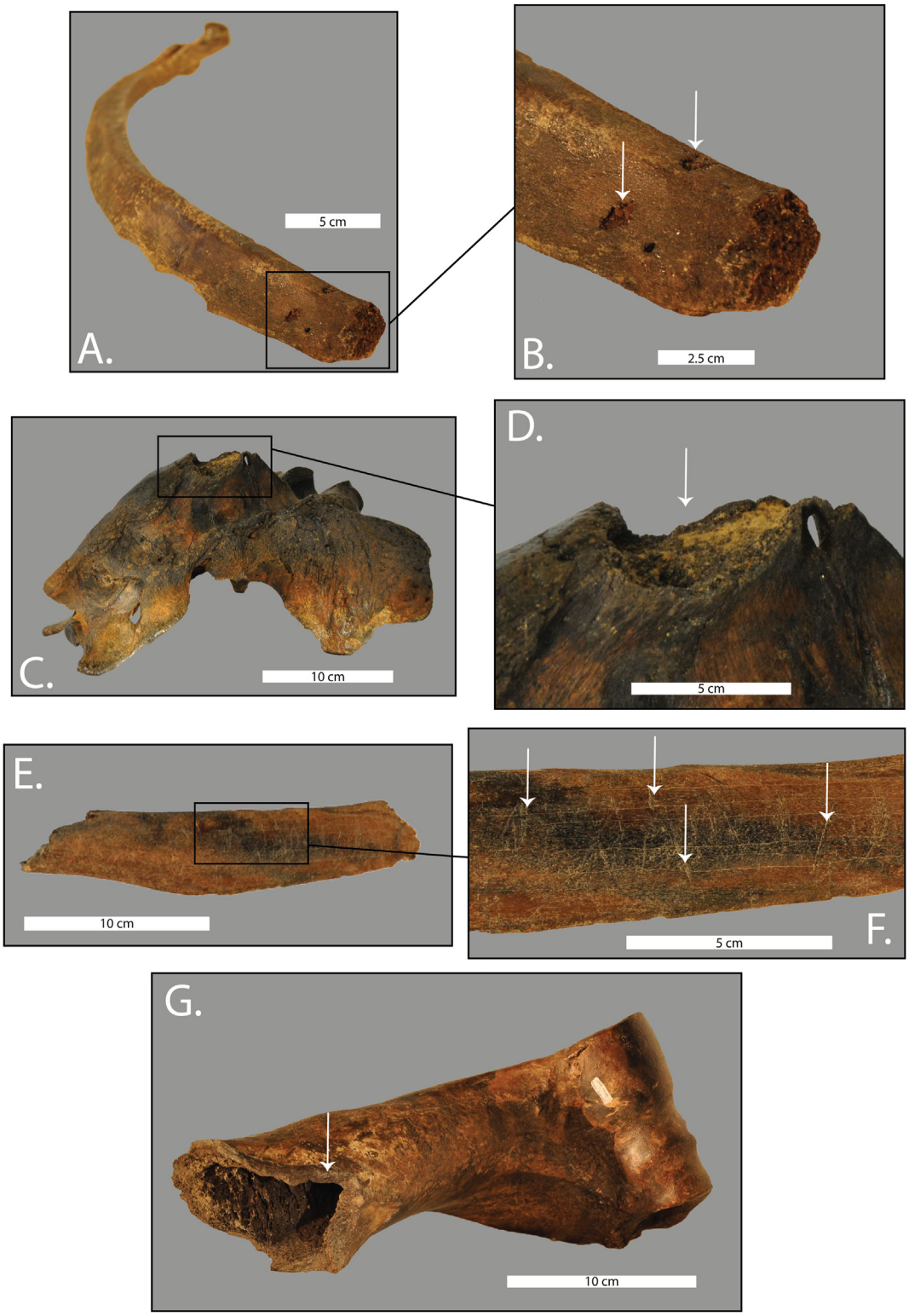

Fig. 10. Sample of Clark Quarry *Bison latifrons* skeletal modifications. A) GCVP 10089; complete right rib. B) Arrows point to tooth puncture marks on distal end of GCVP 10089. C) GCVP 10507; sacrum. D) Arrow points to gnaw marks on anterior-dorsal median sacral crest of GCVP 10507. E) GCVP 19988; rib fragment. F) Arrows point to trample marks on surface of GCVP 19988. G) GCVP 15538; right humerus. Arrow points to a proximal spiral fracture.

flood plain. Furthermore, some limbs unearthed at Clark Quarry were orientated near vertically, suggesting the bones were deposited quickly.

6.2. Age-dating discrepancy

Previously published ages for Clark Quarry were based on ^{14}C from bone and enamel apatite of *M. columbi* and *B. latifrons* (Patterson et al., 2012). While these results agree with our current ^{14}C ages of bison rib bioapatite, they differ significantly from those obtained from our more recent IRSL ages. A limitation of the radiocarbon dating method as applied to carbonate materials, including mollusk shells and carbonate substituted within bone bioapatite, is the possibility of isotopic exchange with carbonates of soil solution groundwater, or atmospheric CO_2 (Cherkinsky, 2009; Zazzo and Saliège, 2011; Zazzo, 2014). The alteration of the mineral (carbonate) fraction of bone, enamel, and shell can involve the precipitation of secondary minerals (calcite) and/or isotopic exchange between structural carbonate and the dissolved inorganic carbon (DIC) in groundwater. Chemical pretreatments are necessary to remove diagenetic, secondary carbonates from bioapatite; however, these methods are not sufficient if the bone bioapatite structure has been degraded completely and exposed to isotope exchange. In the majority of such cases, the altered bone samples tend to give younger, rather than older, ages (Zazzo and Saliège, 2011). The possibility of isotope exchange at Clark Quarry, and likely the ACP in general, is increased due to the combined effects of a fluctuating water table and alternating wet and dry seasons. Thus, radiocarbon dates on carbonate samples, including dates on bone bioapatite, likely underestimate the age of the fossils and should be interpreted as a minimum age estimate.

IRSL ages (including overlap of uncertainty ranges) agree with the stratigraphic position from where they were collected (i.e., the bottom sample is the oldest date and ages of subsequent samples decrease upward). Additionally, all IRSL ages yielded a temporal overlap window from 59.13 to 58.85 ka, which may even suggest a single depositional pulse or rapid aggradation. The luminescence method is not without limitations that can lead to age over- or underestimation. If sediments are transported a short distance, particularly in high energy geomorphic settings and then rapidly buried, the previous signals may not have been fully reset by sunlight prior to deposition. Partial bleaching is the incomplete resetting of a prior signal, and if not properly identified and mitigated through single grain dating and age modelling, this could lead to an age overestimation (e.g., Rittenour, 2008; Rhodes, 2015). Generally, for Holocene-aged deposits, the effects of partial bleaching can lead to substantial residual doses and age overestimates given the low natural doses in young sediments (Olley et al., 1998), while Pleistocene ages are less affected by these small residuals. Additionally, spread in the individual D_E data is low and distributions are largely symmetrical with no tail toward high D_E values (Fig. S1), indicating most grains were fully reset prior to deposition. IRSL measurements can suffer from athermal decay of trapped charges over geologic time, known as fading, and thus IRSL D_Es and ages need to be corrected for this signal loss (e.g., Auclair et al., 2003). We have made laboratory measurements to estimate the degree of fading and results indicate a relatively low and consistent amount of fading can be accounted for (Table 1). Given that the IRSL ages followed stratigraphic agreement and the radiocarbon samples lacked stratigraphic order, which can be explained by carbon isotopic exchange, we rely on the IRSL ages to represent the true age of sediment deposition.

Taken together, the most conservative interpretation of the direct dating methods suggests that the radiocarbon ages provide a minimum age estimate for the fossil-bearing deposit of 20.9–19.3 cal ka BP, while the IRSL ages provide a maximum conservative age estimate of 68–52 ka (rounded to the nearest 1000 yr), with the possibility of further age constraints. Additionally, based on paleoclimatic data discussed below, we suggest that the true age of the fossil deposit is closer to the IRSL ages.

6.3. Comparison of IRSL ages to climate and fluvial models

The Wisconsinan glaciation occurred during MIS 4–2. IRSL ages collected from Clark Quarry and FLETC-1 straddle MIS 4 and 3 (Fig. 8); however, the time window of overlap for all samples (59.13–58.85 ka) occurs within MIS 4. Vandenberghe (1993) developed a periglacial fluvial cycle which describes fluvial style and associated sedimentological and hydrological factors accompanying the climate cycles for both inland and coastal environments. During the IRSL sample overlap window, sea level was estimated to be 80 m lower than present day (Hine et al., 2017); thus, shifting the shoreline 150 km eastward. This in turn would make the fluvial system at Clark Quarry behave as an inland river as opposed to a coastal river. Vandenberghe (1993) suggests that periglacial inland rivers aggrade and switch to a braided fluvial style during mid-glacial cycles because of high peak discharge, high sediment supply, low vegetation density, and cooler temperatures. Evidence of a braided fluvial system proximal to the Clark Quarry site is observed within the DEM, GPR, and textural analysis data (Figs. 1D, 4-6). Furthermore, the IRSL age overlap window may suggest a single event or rapid deposition occurred during MIS 4 (Fig. 8A). Therefore, the morphostratigraphic and geochronologic data complement the Vandenberghe (1993) periglacial fluvial cycle model and its climatic implications. In doing so, it is reasonable to suggest that the age range of IRSL ages for the deposition of the Clark Quarry site can be constrained to 59.13–58.85 ka (MIS 4).

6.4. Morphostratigraphic evolutionary model of Clark Quarry

The multidisciplinary methods utilized in this study allowed for the construction of a morphostratigraphic evolutionary model of Clark Quarry and the surrounding area (Fig. 9). A four-stage morphostratigraphic model was developed using sedimentologic, geomorphic, geophysical, geochronologic, and biologic data.

6.4.1. Stage 1

Stage 1 represents the period when the Princess Anne barrier island formed, 100–80 ka (Wehmiller et al., 2004; Willis, 2006; Doar and Kendall, 2014, Fig. 9A), most likely during the MIS 5c or 5a interglacial. During its formation, the Princess Anne barrier island developed just seaward of the older Pamlico barrier island. Much like the modern barrier islands along the Georgia coast, low-lying estuarine deposits likely separated the two paleobarrier islands (e.g., modern Sapelo and Blackbeard Islands, GA, USA; Oertel, 1979; Hayes, 1994; McBride et al., 2022). Sediment samples collected from Unit 5 (Princess Anne backbarrier) consisted of fine sand. These sediments were likely deposited by a meandering tidal creek environment because of the coarseness of sediment grains, lack of mud, bioturbation (sporadic, localized burrows), abundance of mud snail shells, and fine shell hash within Unit 5 (Seminack and Buynevich, 2013; Seminack and McBride, 2019).

6.4.2. Stage 2

Stage 2 begins as the backbarrier tidal creek transitioned into an inland fluvial system (Fig. 9B). Textural analysis suggests this was an abrupt transition. The boundary between the Princess Anne estuarine sediments and fluvially-derived sediments is defined by a change in color and a sudden increase in grain size. The source sediment for the hypothesized braided stream was likely locally

reworked well-sorted estuarine and barrier-island deposits consisting of fine sand. This would account for the lack of size variation within the fluvially deposited sediment of stratigraphic Unit 4 (Fig. 2B and C, and 6A). This further emphasizes the importance of the sudden increase in grain size at the base of Unit 4. IRSL ages suggest that the change from an estuary to fluvial setting occurred 68.23–58.85 ka (MIS 4), based on the overlap of IRSL samples CQ-19-3 and CQ-19-4 (Fig. 8A). GPR data likely recorded the signature of the fluvial system transitioning from a meandering to braided style (Fig. 5) during this stage. The fluvial system ceased sediment deposition by 52.24 ka (MIS 3, IRSL sample CQ-19-1); however, if the fluvial unit was deposited as a single event, or rapid deposition, the time of deposition can be constrained to 59.13–58.85 ka (MIS 4), based on age uncertainty overlap of IRSL samples CQ-19-1, CQ-19-2, CQ-19-3, and FLETC-OSL-1-19-155cm (Fig. 8). The fluvial unit is interpreted at Clark Quarry as sheet sands from a braided stream (Miall, 1985, 2010). Stage 2 also represents the period where the faunal remains were exposed subaerially for some time, long enough to develop trample- and scavenger gnaw-marks. A subsequent flooding event entrained and buried the faunal remains within the fluvial unit quickly.

6.4.3. Stage 3

Stage 3 occurred as the braided stream waned and flow decreased (Fig. 9C). This stage likely ended by 52.24 ka (MIS 3). The waning of fluvial activity is inferred from the fining-upward trend in sediment grain size, thus indicating a decrease in fluvial energy.

6.4.4. Stage 4

Stage 4 is represented by soil development forming Units 1–3 (Fig. 9D). Soils represent landscape stability and suggest a lack of fluvial activity. The area transitioned into the present-day landscape during Stage 4. Radiocarbon ages suggest that this process began occurring 7 ka at a minimum.

6.5. Larger implications

Fossil deposits in southeastern North America provide a unique window into late-Pleistocene ecosystems in North America due to their removal from glacial conditions that dominate much of this period (Russell et al., 2009). Although the region has a rich history of geologic and paleontologic exploration (e.g., Hulbert and Pratt, 1998; Webb et al., 2006), data from these localities has been challenging to integrate into hypotheses focused on late-Pleistocene paleoecology due to their imprecise temporal context. Given their ubiquity, backbarrier depositional environments along the ACP potentially represent a valuable source of late-Pleistocene paleoecologic data. However, our work highlights the need for closer examination of the effects of diagenesis on the radiocarbon record of these depositional environments, particularly the direct dating of late-Pleistocene aged vertebrate remains, whose ages are likely underestimated due to isotopic exchange with surrounding sediments. Finally, our work highlights the importance of luminescence methods as reliable geochronologic tools in Pleistocene coastal settings of the ACP and elsewhere.

7. Conclusions

A multidisciplinary approach, including sedimentological, geomorphic, geophysical, geochronological, biological, and remote sensing techniques were employed to reconstruct the depositional environment of a well-documented, fossil-rich site in Brunswick, GA, USA, known as Clark Quarry, which yielded late-Pleistocene fossils including *B. latifrons* and *M. columbi*. The fossil-rich sandy unit at Clark Quarry is interpreted to have been deposited by a braided fluvial system active 68.23–52.24 ka, with possible likely further age constraint to 59.13–58.85 ka. Evidence of the fluvial system includes relict channel patterns imaged by a DEM, a stacked channel complex within the shallow subsurface (likely capturing a change from meandering to braided stream style), textural analysis, and paleoflow reconstruction. Post-mortem bone modifications (e.g., carnivore gnaw and trampling marks) identified on *B. latifrons* bones unearthed at Clark Quarry suggest that the organisms were likely exposed subaerially for some time before being disarticulated and entrained by a likely flooding event and quickly buried. A discrepancy in IRSL and ^{14}C ages stresses the importance of utilizing multiple age-dating techniques to identify limitations of each method. In this case, isotopic exchange likely resulted in fossil ages being underestimated by the radiocarbon dating method. Finally, findings from this study demonstrate the important role that fluvial reworking plays in preserved transitional settings (former backbarrier and barrier island environments).

Author statement

Christopher Seminack: Conceptualization, Methodology, Validation, Formal analysis, Investigation, Resources, Data curation, Funding acquisition, Writing – original draft, and Visualization. **Jesse Thornburg**: Conceptualization, Methodology, Investigation, and Writing – review & editing. **Alfred Mead**: Conceptualization, Methodology, Investigation, and Writing – review & editing. **Heidi Mead**: Conceptualization, Investigation, and Writing – review & editing. **Carla Hadden**: Conceptualization, Methodology, Investigation, and Writing – review & editing. **Alexander Cherkinsky**: Conceptualization, Methodology, Investigation, and Writing – review & editing. **Michelle S. Nelson**: Conceptualization, Methodology, Investigation, and Writing – review & editing. **David Patterson**: Conceptualization, Methodology, Investigation, Funding acquisition, and Writing – review & editing

Declaration of competing interest

The authors declare that they have no known competing financial interests or personal relationships that could have appeared to influence the work reported in this paper.

Acknowledgements

This project was supported by the National Geographic Society (NGS-55573R-19) and University of North Georgia Presidential Award (2019). The authors would like to thank the two reviewers of this manuscript, who provided valuable comments and strengthened the manuscript.

Appendix A. Supplementary data

Supplementary data to this article can be found online at https://doi.org/10.1016/j.quascirev.2022.107496.

References

Aitken, M.J., Tite, M.S., Reid, J., 1964. Thermoluminescent dating of ancient ceramics. Nature 202, 1032–1033. https://doi.org/10.1038/2021032b0.

Aitken, M.J., Alldred, J.C., 1972. The assessment of error limits in thermoluminescent dating. Archaeometry 14, 257–267. https://doi.org/10.1111/j.1475-4754.1972.tb00068.x.

Adamiec, G., Aitken, M., 1998. Dose-rate conversion factors: update. Ancient TL 16, 37–50.

Aitken, M.J., 1985. Thermoluminescence Dating. Academic Press, London. https://doi.org/10.1002/gea.3340020110.

Aitken, M.J., 1998. An Introduction to Optical Dating: the Dating of Quaternary Sediments by the Use of Photon-Stimulated Luminescence. Oxford University

Press, New York, p. 267. https://doi.org/10.1017/S0016756899551777.
Aitken, M.J., Xie, J., 1990. Moisture correction for annual gamma dose. Ancient TL 8, 6–9.
Auclair, M., Lamothe, M., Huot, S., 2003. Measurement of anomalous fading for feldspar IRSL using SAR. Radiat. Meas. 37, 487–492. https://doi.org/10.1016/S1350-4487(03)00018-0.
Blair, M., Yukihara, E.G., McKeever, S.W.S., 2005. Experiences with single-aliquot OSL procedures using coarse-grain feldspars. Radiat. Meas. 39, 361–374. https://doi.org/10.1016/j.radmeas.2004.05.008.
Blott, S.J., Pye, K., 2001. GRADISTAT: a grain size distribution and statistics package for the analysis of unconsolidated sediments. Earth Surf. Process. Landforms 26, 1237–1248. https://doi.org/10.1002/esp.261.
Bøtter-Jensen, L., Andersen, C.E., Duller, G.A.T., Murray, A.S., 2003. Developments in radiation, stimulation and observation facilities in luminescence measurements. Radiat. Meas. 37, 535–541. https://doi.org/10.1016/S1350-4487(03)00020-9.
Cherkinsky, A., 2009. Can we get a good radiocarbon age from a “bad bone”? Determining the reliability of radiocarbon age from bioapatite. Radiocarbon 51, 647–655. https://doi.org/10.1017/S0033822200055995.
Cherkinsky, A., Culp, R.A., Dvoracek, D.K., Noakes, J.E., 2010. Status of the AMS facility at the university of Georgia. Nucl. Instrum. Methods Phys. Res. Sect. B Beam Interact. Mater. Atoms 268, 867–870. https://doi.org/10.1016/j.nimb.2009.10.051.
Doar, W., Kendall, C., 2014. An analysis and comparison of observed Pleistocene South Carolina (USA) shoreline elevations with predicted elevations derived from Marine Oxygen Isotope Stages. Quat. Res. 82, 164–174. https://doi.org/10.1016/j.yqres.2014.04.005.
Falconer, H., 1857. On the species of mastodon and elephant occurring in the fossil state of Great Britain. Q. J. Geol. Soc. Lond. 13, 307–360.
Folk, R.L., 1980. *Petrology of Sedimentary Rocks*: Austin. Hemphill Publishing Company, p. 190.
Folk, R.L., Ward, W.C., 1957. Brazos River bar: a study in the significance of grain size parameters. J. Sediment. Petrol. 27, 3–26. https://doi.org/10.1306/74D70646-2B21-11D7-8648000102C1865D.
Frison, G.C., Todd, L.C., 1986. The Colby Mammoth Site: Taphonomy and Archaeology of a Clovis Kill in Northern Wyoming. University of New Mexico Press, Albuquerque, NM.
Galbraith, R.F., Roberts, R.G., 2012. Statistical aspects of equivalent dose and error calculation and display in OSL dating: an Overview and some recommendations. Quat. Geochronol. 11, 1–27. https://doi.org/10.1016/j.quageo.2012.04.020.
Guérin, G., Mercier, N., Adamiec, G., 2011. Dose-rate conversion factors: update. Ancient TL 29, 5–8.
Hanson, C.B., 1980. Fluvial taphonomic processes: models and experiments. In: Behrensmeyer, A.K., Hill, A.P. (Eds.), Fossils in the Making. University of Chicago Press, Chicago, IL, pp. 156–181.
Heaton, T.J., Köhler, P., Butzin, M., Bard, E., Reimer, R.W., Austin, W.E.N., Ramsey, C.B., Grootes, P.M., Hughen, K.A., Kromer, B., Reimer, P.J., Adkins, J., Burke, A., Cook, M.S., Olsen, J., Skinner, L.C., 2020. Marine20—the marine radiocarbon age calibration curve (0–55,000 cal BP). Radiocarbon 62. https://doi.org/10.1017/RDC.2020.68.
Hails, J.R., Hoyt, J.H., 1969a. The significance and limitation of statistical parameters for distinguishing ancient and modern sedimentary environments of the lower Georgia coastal plain. J. Sediment. Petrol. 39, 559–580. https://doi.org/10.1306/74D71CD0-2B21-11D7-8648000102C1865D.
Hails, J.R., Hoyt, J.H., 1969b. An appraisal of the evolution of the lower Atlantic coastal plain of Georgia, U.S.A. Trans. Inst. Br. Geogr. 46, 53–68. https://www.jstor.org/stable/621408.
Hayes, M.O., 1994. The Georgia Bight Barrier System. In: Davis Jr., R.A. (Ed.), Geology of Holocene Barrier Island Systems. Springer-Verlag, Berlin, pp. 233–304. https://doi.org/10.1007/978-3-642-78360-9.
Hine, A.C., Martin, E.E., Jaeger, J.M., Brenner, M., 2017. Paleoclimate of Florida. In: Chassignet, E.P., Jones, J.W., Mirsa, V., Obeysekera, J. (Eds.), Florida's Climate. Florida Climate Institute, Gainesville, FL, pp. 105–138. http://purl.flvc.org/fsu/fd/FSU_libsubv1_scholarship_submission_1515511145_a2730749.
Hoyt, J.H., Hails, J.R., 1967. Pleistocene shoreline sediments in coastal Georgia: deposition and modification. Nature 155, 1541–1543. https://www.science.org/doi/abs/10.1126/science.155.3769.1541.
Hoyt, J.H., Henry Jr., V.J., Weimer, R.J., 1968. Age of late-Pleistocene shoreline deposits, coastal Georgia. International Association for Quaternary Research 8, 381–393.
Hulbert, R.C., Pratt, A.E., 1998. New Pleistocene (Rancholabrean) vertebrate faunas from Coastal Georgia. J. Vertebr. Paleontol. 18, 412–429. https://doi.org/10.1080/02724634.1998.10011069.
Huntley, D.J., Godfrey-Smith, D.I., Thewalt, M.L.W., 1985. Optical dating of sediments. Nature 313, 105–107. https://doi.org/10.1038/313105a0.
Huntley, D.J., Baril, M.R., 1997. The K content of the K-feldspars being measured in optical dating or in the thermoluminescence dating. Ancient TL 15, 11–13.
Huntley, D.J., Hancock, R.G.V., 2001. The Rb contents of the K-feldspar grains being measured in optical dating. Ancient TL 19, 43–46.
Huntley, D.J., Lamothe, M., 2001. Ubiquity of anomalous fading in K-feldspars and the measurement and correction for it in optical dating. Can. J. Earth Sci. 38, 1093–1106. https://doi.org/10.1139/e01-013.
Ivester, A.H., Leigh, D.S., 2003. Riverine dunes on the coastal plain of Georgia, U.S.A. Geomorphology 51, 289–311. https://doi.org/10.1016/S0169-555X(02)00240-4.
Kurtén, B., Anderson, E., 1980. Pleistocene Mammals of North America. Columbia University Press, New York, NY, p. 442.
Lawton, D.E., Moye, F.J., Murray, J.B., O'Connor, B.J., Penley, H.M., Sandrock, G.S., Marsalis, W.E., Friddell, M.S., Hetrick, J.H., Huddlestun, P.F., Hunter, R.E., Mann, W.R., Martin, B.F., Pickering, S.M., Schneeberger, F.J., Wilson, J.D., 1976. Geologic map of Georgia, Georgia Dept. of Natural Resources, Geologic and Water Resources division. Georgia Geological Survey. Scale 1:500,000.
Leigh, D.S., 2006. Terminal Pleistocene braided to meandering transition in rivers of the southeastern USA. Catena 66, 155–160. https://doi.org/10.1016/j.catena.2005.11.008.
Leigh, D.S., 2008. Late Quaternary climates and river channels of the Atlantic coastal plain, southeastern USA. Geomorphology 101, 90–108. https://doi.org/10.1016/j.geomorph.2008.05.024.
Leigh, D.S., Srivastava, P., Brook, G.A., 2004. Late Pleistocene braided rivers of the Atlantic coastal plain, USA. Quat. Sci. Rev. 23, 65–84. https://doi.org/10.1016/S0277-3791(03)00221-X.
Lisiecki, L.E., Raymo, M.E., 2005. A Pliocene-Pleistocene stack of 57 globally distributed benthic $\delta^{18}O$ records. Paleoceanography 20. https://doi.org/10.1029/2004PA001071.
Lyell, C., 1849. A Second Trip to the United States of North America, vol. 1. Harper and Brothers, New York, NY, p. 273.
Lyman, R.L., 1994. Vertebrate Taphonomy. Cambridge University Press, Cambridge, England, p. 524.
Martin, R.E., 1999. Taphonomy a Process Approach. Cambridge University Press, Cambridge, England, p. 508.
Mead, A.J., Bahn, R.A., Chandler, R.M., Parmley, D., 2006. Preliminary comments on the Pleistocene vertebrate fauna from Clark Quarry, Brunswick, GA. Curr. Res. Pleistocene 23, 174–176.
McBride, R.A., Anderson, J.B., Buynevich, I.V., Byrnes, M.R., Cleary, W., Fenster, M.S., FitzGerald, D.M., Hapke, C.J., Harris, M.S., Hein, C.J., Johnson, C.L., Klein, A.H.F., Liu, B., de Menezes, J.T., Mulhern, J.S., Oliver, T.S.N., Pejrup, M., Riggs, S.R., Roberts, H.H., Rodriquez, A.B., Seminack, C.T., Short, A.D., Stone, G.W., Tamura, T., Wallace, D.J., Wang, P., 2022. Morphodynamics of Modern and Ancient Barrier Systems: An Updated and Expanded Synthesis. In: Shroder, J. (Ed.), Treatise on Geomorphology, vol. 8. Elsevier, Academic Press, pp. 289–417. https://doi.org/10.1016/B978-0-12-818234-5.00153-X in chief.
Mejdahl, V., 1979. Thermoluminescence dating: Beta-dose attenuation in quartz grains. Archaeometry 21, 61–72. https://doi.org/10.1111/j.1475-4754.1979.tb00241.x.
Miall, A., 2010. Alluvial deposits. In: James, N.P., Dalrymple, R.W. (Eds.), Facies Models 4. Geological Association of Canada, St. John's, NL, pp. 105–138.
Miall, A., 1985. Architectural-element analysis: a new method of facies analysis applied to fluvial deposits. Earth Sci. Rev. 22, 261–308. https://doi.org/10.1016/0012-8252(85)90001-7.
National Oceanic and Atmospheric Administration (NOAA), 2021. Tides and Currents. https://tidesandcurrents.noaa.gov. (Accessed 12 August 2021). Accessed date.
Noble, E.J., McManus, J.G., Mead, A.J., Mead, H., Seminack, C.T., Baco, W., Bennett, T., Crain, N.M., Duckworth, C., Malasek, T., Pearson, J.Z., Rhinehart, P., Ussery, M.E., Sun, Y., Patterson, J.R., Patterson, D.B., 2020. Enamel isotopes reveal late Pleistocene ecosystem dynamics in southeastern North America. Quat. Sci. Rev. 236, 106284. https://doi.org/10.1016/j.quascirev.2020.106284.
Oertel, G.F., 1979. Barrier island development during the Holocene Recession, southeastern United States. In: Barrier Islands from the Gulf of St. Lawrence to the Gulf of Mexico. Academic Press, New York, pp. 273–290.
Olley, J., Caitcheon, G., Murray, A., 1998. The distribution of apparent dose as determined by optically stimulated luminescence in small aliquots of fluvial quartz: implications for dating young sediments. Quat. Sci. Rev. 17, 1033–1040. https://doi.org/10.1016/S0277-3791(97)00090-5.
Patterson, D.B., Mead, A.J., Bahn, R.A., 2012. New skeletal remains of *Mammuthus columbi* from Glynn County, Georgia with notes on their historical and paleoecological significance. SE. Nat. 11, 163–172. https://doi.org/10.1656/058.011.0201.
Parmley, D., Clark, J.L., Mead, A.J., 2020. Amphibians and squamates from the Late Pleistocene (Rancholabrean) Clark Quarry, Coastal Georgia. Eastern Paleontologist 7, 1–23.
Prescott, J.R., Hutton, J.T., 1994. Cosmic ray contributions to dose rates for luminescence and ESR dating. Radiat. Meas. 23, 497–500. https://doi.org/10.1016/1350-4487(94)90086-8.
Ramsey, C.B., 2021. OxCal Program, Version 4.4.
Rees-Jones, J., 1995. Optical dating of young sediments using fine-grain quartz. Ancient TL 13, 9–14.
Reimer, P., Austin, W.E.N., Bard, E., Bayliss, A., Blackwell, P.G., Ramsey, C.B., Butzin, M., Cheng, H., Edwards, R.L., Friedrich, M., Grootes, P.M., Guilderson, T.P., Hajdas, I., Heaton, T.J., Hogg, A.G., Hughen, K.A., Kromer, B., Manning, S.W., Muscheler, R., Palmer, J.G., Pearson, C., van der Plicht, J., Reimer, R.W., Richards, D.A., Scott, E.M., Southon, J.R., Turney, C.S.M., Wacker, L., Adolphi, F., Büntgen, U., Capano, M., Fahrni, S., Fogtmann-Schulz, A., Friedrich, R., Köhler, P., Kudsk, S., Miyake, F., Olsen, J., Reinig, F., Sakamoto, M., Sookdeo, A., Talamo, S., 2020. The IntCal20 Northern Hemisphere radiocarbon age calibration curve (0–55 cal kBP). Radiocarbon 62. https://doi.org/10.1017/RDC.2020.41.
Rhinehart, P.D., 2021. A Late Pleistocene Herpetofauna from Clark Quarry, Glynn County, Georgia. M. S. Thesis. Milledgeville, Georgia College and State University, p. 51.
Rhodes, E.J., 2015. Dating sediments using potassium feldspar single-grain IRSL: initial methodological considerations. Quat. Int. 362, 14–22. https://doi.org/

10.1016/j.quaint.2014.12.012.
Rittenour, T.M., 2008. Luminescence dating of fluvial deposits: applications to geomorphic, palaeoseismic and archaeological research. Boreas 37, 613–635. https://doi.org/10.1111/j.1502-3885.2008.00056.x.
Russell, D.A., Rich, F.J., Schneider, V., Lynch-Stieglitz, J., 2009. A warm thermal enclave in the Late Pleistocene of the South-eastern United States. Biol. Rev. 84, 173–202. https://doi.org/10.1111/j.1469-185X.2008.00069.x.
Seminack, C.T., Buynevich, I.V., 2013. Sedimentological and geophysical signatures of a relict tidal inlet complex along a wave-dominated barrier: Assateague Island, Maryland, U.S.A. J. Sediment. Res. 83, 132–144. https://doi.org/10.2110/jsr.2013.10.
Seminack, C.T., McBride, R.A., 2019. New perspectives on the geomorphic, sedimentologic, and stratigraphic signatures of former wave-dominated tidal inlets: Assateague Island, Maryland, U.S.A. J. Sediment. Res. 89, 312–334. https://doi.org/10.2110/jsr.2013.10.
Shipman, P., 1993. Life History of a Fossil: an Introduction to Taphonomy and Paleoecology. Harvard University Press, Cambridge, MA, p. 232.
Soil Survey Staff, 2014. Keys to Soil Taxonomy, twelfth ed. USDA-Natural Resources Conservation Service, Washington, D.C.
Thomas, D.H., 2008. Native American Landscapes of St. Catherines Island, Georgia II. The Data, American Museum of Natural History #88, pp. 343–831. Part II.
Toots, H., 1965a. Orientation and distribution of fossils as environmental indicators. In: Bitter, R.K., De Voto, R.H. (Eds.), Nineteenth Field Conference of the Wyoming Geological Association. Wyoming Geological Association, Casper, WY, pp. 219–229.
Toots, H., 1965b. Random orientation of fossils and its significance. Rocky Mt. Geol. 4, 59–62.
Vandenberghe, J., 1993. Changing fluvial processes under changing periglacial conditions. Z. Geomorphol. 88, 17–28.
Voorhies, M.R., 1969. Taphonomy and Population Dynamics of an Early Pliocene Vertebrate Fauna, Knox County, Nebraska. University of Wyoming Contributions to Geology Special Paper No. 1, Laramie, WY.
Voorhies, M.R., 1971. The Watkins Quarry: A new Late Pleistocene mammal locality in Glynn County, Georgia. Bull. Ga. Acad. Sci. 29, 128.
Ward, W.T., Ross, P.J., Colquhoun, D.J., 1971. Interglacial high sea levels – an absolute chronology derived from shoreline elevations. Palaeogeogr. Palaeoclimatol. Palaeoecol. 9, 77–99. https://doi.org/10.1016/0031-0182(71)90034-4.
Wallinga, J., Murray, A., Wintle, A., 2000. The single-aliquot regenerative-dose (SAR) protocol applied to coarse-grain feldspar. Radiat. Meas. 32, 529–533. https://doi.org/10.1016/S1350-4487(00)00091-3.
Webb, S.D., Graham, R.W., Barnosky, A.D., Bell, C., Franz, R., Hadly, E.A., Lundelius, E., McDondald, H., Martin, R., Semken, H., Steadman, D.W., 2006. Vertebrate Paleontology. In: First Floridians and Last Mastodons: the Page-Ladson Site in the Aucilla River. Springer, Dordrecht.
Wehmiller, J.F., Simmons, K.R., Cheng, H., Edwards, R.L., Martin-McNaughton, J., York, L.L., Krantz, D.E., Chun-Chou, S., 2004. Uranium-series coral ages from the US Atlantic coastal plain—the “80 ka problem” revisited. Quat. Int. 120, 3–14. https://doi.org/10.1016/j.quaint.2004.01.002.
Wintle, A.G., 1997. Luminescence Dating: Laboratory Procedures and Protocols. Radiat. Meas. 27, 769–817. https://doi.org/10.1016/S1350-4487(97)00220-5.
Willis, R.A., 2006. Genetic Stratigraphy and Geochronology of Last Interglacial Shorelines of the Central Coast of South Carolina. Masters Thesis. Louisiana State University, Baton Rouge, p. 126.
Zazzo, A., 2014. Bone and enamel carbonate diagenesis: a radiocarbon prospective. Palaeogeogr. Palaeoclimatol. Palaeoecol. 416, 168–178. https://doi.org/10.1016/j.palaeo.2014.05.006.
Zazzo, A., Saliège, J.F., 2011. Radiocarbon dating of biological apatites: a review. Palaeogeogr. Palaeoclimatol. Palaeoecol. 310, 52–61. https://doi.org/10.1016/j.palaeo.2010.12.004.